Controlled Patterning of Diblock Copolymers by Monolayer Langmuir−Blodgett Deposition

S. M. Baker,* K. A. Leach, C. E. Devereaux, and D. E. Gragson†

Department of Chemistry, 301 East 12th Street, Harvey Mudd College, Claremont, California 91711

Received December 3, 1999; Revised Manuscript Received May 22, 2000

ABSTRACT: Nonlithographic techniques for patterning structures on the nanometer scale can provide methods for direct control of particle spacing at surfaces. By using diblock copolymers, the surface density of a film can be established by the properties and area of the anchoring block, and the feature sizes can be set through the choice of free block dimensions. By depositing poly(styrene)−poly(ethylene oxide) (PS−PEO) diblock copolymers of different fractional composition of PEO on a surface by a Langmuir−Blodgett technique at different pressures, we show that the surface density of poly(styrene) aggregates can be controlled. The separation of PS aggregates on the surface is ensured by selection of the PEO composition so that its projected area is greater than that of the PS for all pressures less than that of the transition from a 2-dimensional to 3-dimensional film. The areal density of these resultant PS surface micelles can be tuned for a particular polymer composition and is linearly dependent on the deposition pressure which defines the region chosen on the phase diagram.

Introduction

Controlled patterning of polymer monolayers on surfaces on very small scales is useful to many applications.[1−3] In many self-assembling diblock copolymer systems at interfaces, an anchoring block defines a minimum packing density, and the geometry of the free block provides surface structure. Patterns are generated when the microphase segregation of the free polymer is driven through the choice of solvent and/or grafting or adsorption density.[4] Arrays of "pinned micelles" of a fairly uniform size and spacing can be created by attaching the ends of homopolymers to a surface by chemical grafting,[5] spin-coating incompatible diblocks on a surface,[6] or adsorbing diblocks from a selective solvent.[7,8] In such systems, the tethering density and the thermodynamic stability of the free block in the solvent used, usually a poor solvent or air, drive the patterning. In such solvents, the adsorbing or tethering block is assumed to be uniformly distributed over the surface, and the resultant surface structures arise from the favorable interactions between the free blocks and the unfavorable stretching away from the entropically favored unconstrained geometry.[9,10]

Our work focuses on the controlled deposition of diblock copolymers on silicon substrates using a Langmuir−Blodgett (LB) trough, where the surface density is a selectable parameter. The history of using the LB trough to build well-ordered films is well established,[11] and the mean molecular area (mmA) is controlled by lateral compression of the film between two barriers. The architecture of the aqueous surface layer can generally be maintained by subsequent deposition of the film on a submerged substrate. Using poly(ethylene oxide)-*b*-poly(styrene), PS−PEO, an amphiphilic copolymer, we can control the spacing between polystyrene aggregates.[12] The PEO block spreads at the air−water interface. When the relative area of the PS block is small, the PS acts as a water-insoluble buoy block at the air−water interface and provides surface structure at the air−solid interface.[13] By selecting the relative molecular weights of the blocks and the deposition pressure, we can ensure that the PS blocks do not interfere with the PEO compression. Patterned spacing is achieved by choosing the pressure and mmA of deposition to a silicon substrate.

Earlier studies of the formation of aggregates upon deposition of polyelectrolyte diblocks[14] and of nonionic diblocks[15] on the surface of the air−water interface suggested that PS forms surface micelles which can be deposited at a solid−liquid interface. In comprehensive studies, Zhu et al.[16,17] described the 2-dimensional analogues to the 3-dimensional spherical, cylindrical, and lamellar micelles as starfish, rod, and planar, respectively, for amphiphilic diblock copolymers at the surface and use the term "jellyfish" for the description of the 3-dimensional micellar structures. This geometrical interpretation was verified by neutron reflectivity measurements.[18,19]

Interesting approaches to patterning have involved deposition of micelles on a surface using an LB trough or by self-assembly. Nonionic diblocks of comparable size hydrophobic and hydrophilic units[15] have been observed to form uniform arrays upon deposition. Polyelectrolyte diblocks have been used to control the spacing[17] between micelles by selection of polymer size, charge, and asymmetry. Recently, arrays of diblock aggregates have been prepared by allowing well-ordered self-assembly of micelles from solutions of varying concentrations.[20] However, direct control of the spacing between the micelles for a particular nonionic polymer diblock has not been easy to achieve. Our approach to control the lateral frequency and size of the aggregates is to establish deposition parameters on the LB trough which allow tunable spacing for a given diblock copolymer. For predominantly hydrophilic PS−PEO diblocks, the spacing between PS aggregates is observed to be a function of deposition pressure. The resulting patterns and periodicity can be manipulated in a straightforward manner by depositing the film under conditions of the desired mmA on the two-dimensional phase diagram.

* To whom correspondence should be addressed. E-mail: shenda_baker@hmc.edu.

† Current address: Department of Chemistry and Biochemistry, Cal Poly State University, San Luis Obispo, CA 93407.

10.1021/ma992029x CCC: $19.00
Published on Web 06/28/2000

Table 1. Properties of Polymers Used[a]

PS-PEO MW (g/mol)	wt %PEO	M_w/M_n	MW_{PEO} (g/mol)	MW_{PS} (g/mol)	*N* of PS	*N* of PEO
250 300	15.5	1.15	39 000	211 500	2034	882
200 000	60	1.28	120 000	80 000	769	2727
375 000	92	1.20	345 000	30 000	288	7840

[a] Data provided by Polymer Laboratories.

Experimental Section

Polymers and Compression Isotherms. Diblock copolymers of PS−PEO were purchased from Polymer Laboratories, Amherst, MA, and the specifications are shown in Table 1. The polymers were chosen so that the limiting area of the PEO pancake in all experiments was bigger than the projected PS area. All surface pressure vs mean molecular area isotherms were collected with a KSV-5000 Langmuir−Blodgett trough with two sliding barriers contained in a clean room of class 5000 at ∼21 °C. Spreading solution of the polymers ranged from 0.5 to 1.2 mg/mL in HPLC chloroform from Spectrum Labs. Concentration in this range had no effect, and little effect is observed for concentrations between 0.1 and 1.5 mg/mL for all films >∼10% PEO. The barriers were compressed at a speed of 1.0 cm/min (20 cm^2/min), and the surface tension was measured using a roughened platinum Wilhelmy plate. The limiting PEO pancake area was determined by extrapolating the steep part of the compression isotherm, π−mmA, at large mmA to $\pi = 0$. The 2-D to 3-D transition (pancake−brush) mmA was determined from the intersection of the line defining the plateau and the extrapolation line.

Film Deposition and Imaging. The substrates were ∼1 cm diameter silicon (111) wafers, sonicated in chloroform for 20 min and ozonated in a Jelight ozone generator for up to 1 h. The silicon was submerged beneath the water surface prior to depositions using the same concentration spreading solutions as used in for the isotherms. The barriers were compressed at 1.0 cm/min to the target pressure, the film was allowed to equilibrate a minimum of 10 min, and the deposition upstroke was 0.5 mm/min. Film transfer ratios were ∼1.0 for all films. Prepared films were allowed to dry overnight and imaged at ambient conditions using a Nanoscope multimode AFM in tapping mode (Digital Instruments, Santa Barbara, CA). Cantilevers purchased from Digital Instruments were 125 μm long with a resonance frequency of ∼260−320 Hz. The lateral scan frequency was typically 1−2 Hz. The images were only plane fit with no other alterations. Comparable images were obtained for multiple films indicating reproducible depositions, except for those indicated in the text.

Results and Discussion

Effective Block Dimensions. Figure 1a shows the compression isotherms for the three different molecular weight polymers. The regions in the compression isotherms illustrate effects of the observed phases and transitions on the liquid interface. At large mmA the surface-active PEO adopts a maximal two-dimensional "pancake" configuration as the PEO block spreads at the interface. The pressure increases rapidly as $\pi \propto \Gamma^3$ (where $\Gamma = 1/\text{mmA}$) at very large mmA as predicted.[21] As the film is compressed laterally, the PEO monomer surface density is increased, raising the surface pressure as the mmA decreases. At the mmA associated with the onset of the phase transition from two to three dimensions, the pancake to brush transition, the PEO monomer density on the surface exceeds a critical concentration. The PEO extends into the subphase, increasing the hydrogen bonding in an exothermic dissolution.[22] This phase transition results in a plateau at constant π of ∼10 mN/m over a large range of mmA, spanning 3 orders of magnitude for the 375K polymer. The plateau, indicative of the first-order transition,[23] continues until either the PEO reaches its limiting brush mmA or the PS at the surface begins to overlap, causing a depletion of PEO at the water−PS interface.[24] In either case, a sharp rise in π is observed. This overlapping of incompressible PS globules at the surface can hinder the brushing of the PEO at both air−water and solvent−water interfaces for mmA approaching that of the PS.[25]

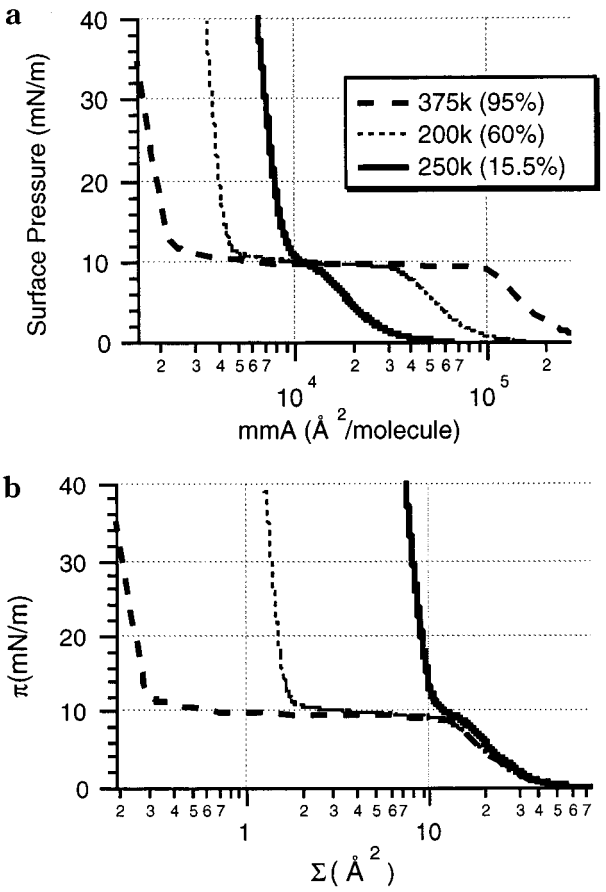

Figure 1. (a) Compression isotherms for three PS−PEO diblock copolymers with % PEO indicated on the graph. Surface pressure, π, is the difference between the surface tension of the neat water subphase (18.2 MΩ·cm) and the surface tension of the film−water interface, $\gamma_0 - \gamma$. A complete isotherm required two to three overlapping measurements in order to obtain the complete range of areas. The isotherms are reproducible to within 1% in the direction of compression. (b) Compression isotherms normalized to the unit area of the PEO monomer.

The differences between the three compression isotherms of Figure 1a reflect the different asymmetries of the polymers used and the different magnitudes of PEO sizes and PS to PEO area ratios. Thus, the 250K polymer with 15.5% PEO does not exhibit a significant plateau in the compression isotherm since the PS is large enough to interfere with the brushing of the PEO and due to the repulsive effect[23] of PS on PEO at the air−water interface. This effect is particularly well illustrated in Figure 1b where a pseudoplateau is observed. The limiting pancake area is unaffected by the PS for this range of asymmetries, and the slope of the curves and plateau for the larger PEO% collapse to a universal curve for π below the phase transition, in agreement with the observations of Fauré et al.[24] The height of the plateau is independent of N_{PEO} and for these asymmetries also of N_{Ps} because of the small PS block.

Table 2. Limiting Areas (Å²/PEO Monomer) Measured with Compression Isotherms[a] and Average Aggregation Number for Each Composition

monomer area (Å²)	250.3K, 15.5% PEO	200K, 60% PEO	375K, 92% PEO
pancake	30	29	28
pancake−brush	16	13	15
Agg #[b]	235 ± 13	95 ± 18	35 ± 5

[a] The comparable limiting values from the literature are 27 and 20 Å² for the pancake and pancake−brush, respectively. The PS area cannot be measured as the PEO limiting brush is reached before the PS globule limiting area is attained. Measured values are reproducible to within ~2%. [b] The average aggregation number (Agg #) is calculated by dividing the number of molecules/unit area as deposited on the LB trough by the average particle density as measured by AFM.

The molecular dimensions empirically determined for the PS and PEO homopolymers are found to be quite useful for establishing the effective areas of both blocks of the diblock at the air/water interface. Kumaki[26] studied very dilute solutions of PS homopolymers and determined that the limiting areas of the monomolecular particles of PS were linearly proportional to the molecular weight according to the relationship $A_0 = 0.04$ M where A_0 is in Å²/molecule and M is the molecular weight. Gonçalves da Silva et al.[22] examined PEO tethered to the air−water interface by a small PS block to determine the limiting areas of PEO phase transitions. They determined that the free area of the monomer is 27 Å² in the "pancake" region determined by extrapolation of the isotherm to the $\pi = 0$ axis. The onset of the transition from two to three dimensions occurs at ~20 Å²/monomer, the limiting pancake to brush mmA. For the larger PEO compositions, the calculations predict that the PS area is almost 25 times smaller than the PEO pancake for the 200K PS−PEO polymer (60% PEO) and 2 orders of magnitude smaller for the 375K PS−PEO polymer (92% PEO). Since the PEO block is so large in these latter polymers, the PEO limiting brush area is reached upon compression before PS overlap. The plateau regions in the isotherms of Figure 1a are consistent with the geometric scaling of the projected block areas.

From the compression isotherms, the mean area per molecule and per monomer were determined as a function of film pressure. These measured values are shown in Table 2. The limiting pancake areas are in good agreement with the empirical observations of Gonçalves da Silva,[22] slightly larger than expected for moderate molecular weight polymers. The PEO pancake to brush area is expected to be 20 Å²/monomer, as determined[22] for $N_{PEO} = 90-445$. Our measured values are significantly below this value. The general overall reduction in area is likely the result of increased entanglement of the PEO for our chains with $N_{PEO} > 800$. It is interesting to note, however, that a monotonic *decrease* in PEO monomer area for increasing PEO is not observed. In our system, the increase in N_{PEO} also corresponds to a decrease in aggregate number and PS fractional coverage. The measured ratio of the PS/PEO area at the onset of the pancake−brush transition is 26%, 10%, and 1.4% for the 15.5%, 60%, and 92% compositions, respectively. Entanglement of PS from different chains in the micelle and the repulsive effect of PS at the interface forces some of the PEO monomers beneath the aggregate to desorb prior to the transition, reducing the measured area per PEO monomer. This effect results in an *increase* in monomer area for the larger PEO number, competing with the entanglement effect of the PEO chains. This repulsive effect of PS is also manifested in its increasing influence on the extent of the plateau in Figure 1b for the larger PS composition diblocks. Because the depositions are done at pressures below the plateau, the effects of PS at the interface have minimal consequences on the patterning.

Film Morphology and Polymer Aggregation. The limiting PEO pancake at the air−water interface is approximately equal to the projected area of the PS globule in air at nominally 8% PEO by molecular weight. For the Langmuir−Blodgett depositions, we have chosen to work with polymers having PEO composition greater than 15%, where spreading solution concentration has minimal effect. We deposit films at surface pressures below the pancake to brush transition where the PS acts as a large tether but should not have continuous overlap at the surface. In this regime, the PEO is a dilute quasi-self-similar adsorbed layer and deposits with a transfer ratio of nearly 1, reproducibly.

Selections of AFM images of all three polymer compositions taken of films deposited at increasing π are shown in Figure 2a,b. For all three polymers, the spacing between the features decreases as the deposition pressure increases, as expected. The surface features in all of these films show a remarkable uniformity in size and shape as well as being fairly uniformly distributed over the surface. The patterns at low surface coverage for the 250K (15.5% PEO) polymer of Figure 2a show the tendency for the aggregates to arrange in strings, an effect that may be consistent with isobaric compression lines on the trough. This observation is not discernible for the 200K (60% PEO) and 375K (92% PEO) films shown in Figure 2b. Furthermore, since the films are all deposited in the dilute regime below the phase transition, no overlap of the PEO is expected and no unusual roughness of the PEO layer is observed in the AFM images.

The measured areas of the surface features observed in Figure 2 are larger than the expected values[26] for the monomolecular particles in every case. We observe that the aggregation number for a particular diblock asymmetry, shown in Table 2, is constant over the entire range of deposition pressures, indicating that the aggregates neither converged to form larger aggregates nor dissociated in this regime. While the aggregation number is independent of the deposition pressure, it is observed to be linearly dependent on the percent PEO where Agg # $= 250 - 2.4 \times$ (% PEO) for this range of concentrations. This relation applies only for PEO compositions greater than ~10% where, ideally, the PS globules would not be in contact before the pancake to brush transition. In practice, this percentage ensures that aggregation produces isolated surface micelles rather than continuous strings or islands. These values of aggregation number are consistent with the variable aggregation numbers observed for nonionic diblocks[14,15] and larger than the polyelectrolyte diblocks as expected due to their repulsive ionic interactions.[27]

The process of aggregate formation is interesting. Apparently, there is a competition between the spreading of the molecules at the interface and the evaporation of the spreading solvent. Entanglement, including polymer interactions in the spreading solvent or from rapid evaporation of solvent after spreading, results in aggregation. The dynamic light scattering results of Gonçalves da Silva et al.[28] show complex autocorrelation traces suggestive of a distribution of aggregate sizes

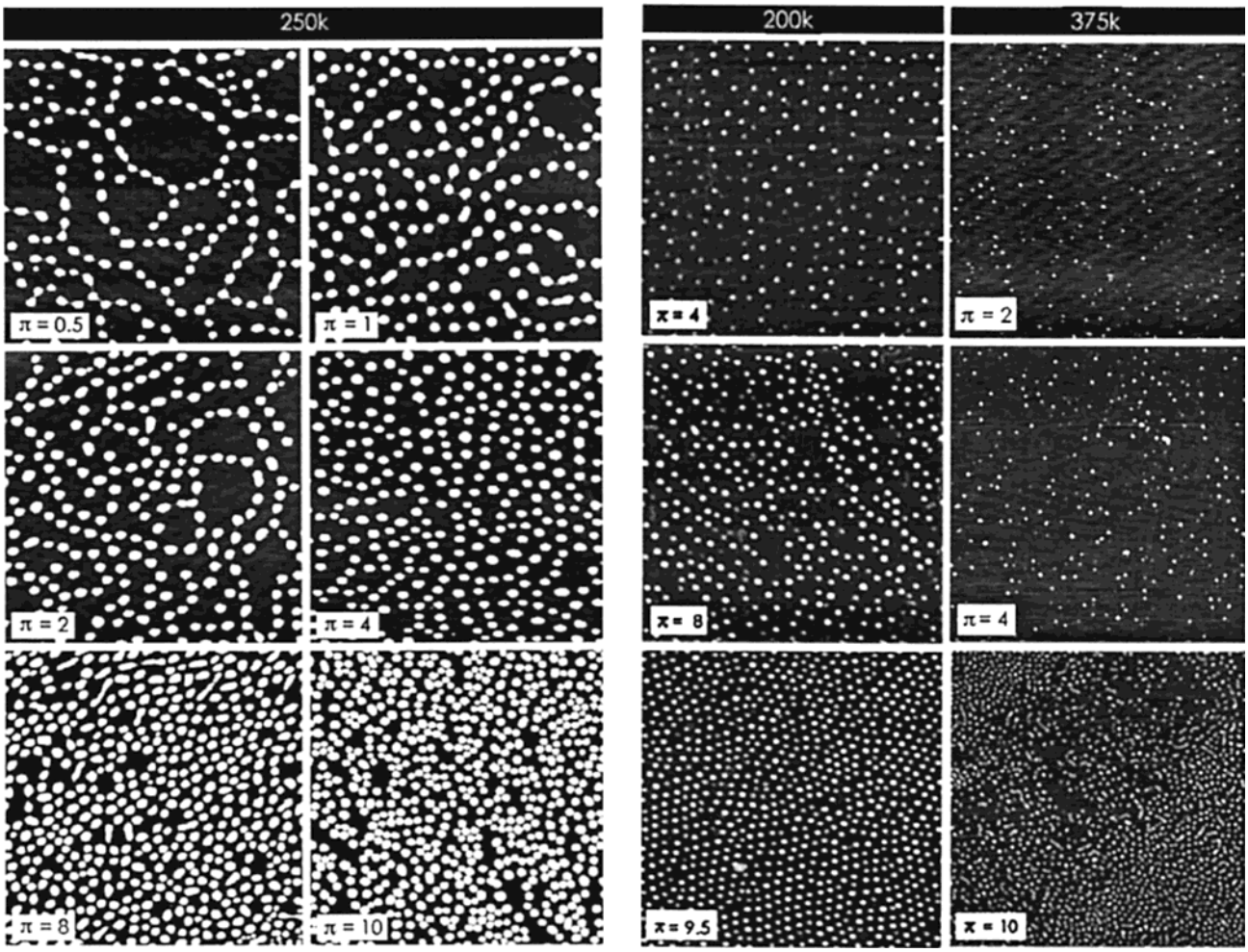

Figure 2. Tapping-mode AFM images (a, left) of the 250.3K PS−PEO diblocks with 15.5% PEO and (b, right) of the 200K and 375K PS−PEO diblocks with 60 and 92 wt % PEO, respectively. All images are 4.0 μm × 4.0 μm with height scales shown as a gray scale. The average heights of the features are 17, 7, and 4 nm, respectively. The deposition pressure is noted on each image and corresponds to an average mmA as determined from the isotherm represented Figure 1. Separate depositions resulted in comparable images, confirming the reproducibility of the films.

whose dimensions increase with increasing N_{PEO}. Our surface features have very uniform size distribution, so solution aggregation may account for some, but not all, of the final aggregation numbers observed at the solid−air surface.

Controlled Patterning of PS Features. The images in Figure 2 show that the pattern spacing of the PS aggregates can be controlled by selecting the deposition pressure. The average particle density as a function of this pressure is shown in Figure 3a. The curve is nearly linear, suggesting that the architecture of the film at the surface of the water is not significantly changed upon deposition on the solid substrate. Deviations from the linearity are expected for depositions near the 10 mN/m plateau as the feedback mechanism during the deposition process maintains a constant pressure, corresponding to a wide range of polymer mmA's. Since we choose our deposition pressures to be below the transition pressure, we have excellent control of the spacing due to the reproducibility of the isotherm in the 2-D region as shown in Figure 2b.

The average aggregate area as a function of PEO composition generally decreases slightly as the density and pressure increase. Figure 3b indicates that while the 60% and 92% PEO polymers produce PS aggregate areas that are well predicted by a simple multiplication of Agg# by Kumaki's empirical observations, the 15.5% PEO polymer with the largest aggregation number produces an area significantly less than predicted. Assuming a spherical PS aggregate, the calculated height would be 27, 17, and 4 nm for the 15.5%, 60%, and 92% PEO compositions, respectively. The increased similarity to the calculation as the aggregation number decreases suggests that connectivity of the PS to the PEO requires the bigger aggregates to have junction points far away from the center of the micelle. Consequently, the entangled PS blocks at the periphery of a large micelle are stretched and may appear with the resolution of the AFM to be flat, resulting in an apparent smaller block. Mass could be conserved with this smaller area by forming a taller PS aggregate; however, the measured heights are less than 20 nm, supporting the above interpretation.

It is interesting to note that while the particle area decreases as particle density increases, the aggregate number in Table 2 remains the same for a given polymer composition, regardless of the deposition pressure. Upon reducing the area of the PEO, the PS is less stretched and the measured area decreases. This observation suggests that the structures are formed upon spreading the solution at the surface with evaporation of solvent and do not rearrange upon compression. Even at pressures greater than 10 mN/m individual aggregates remain, suggesting that the structures formed upon

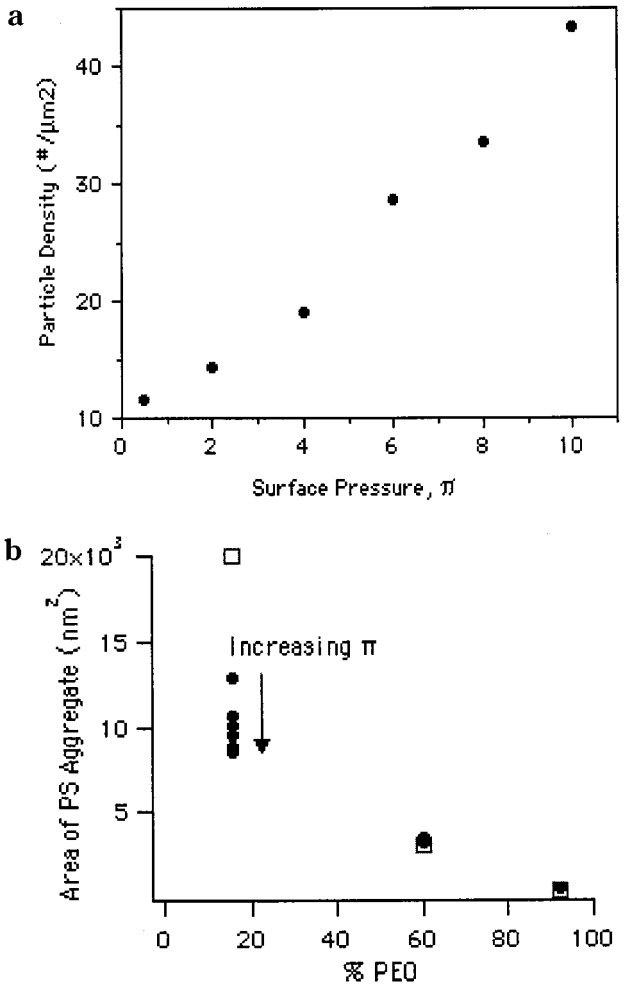

Figure 3. Graph of (a) the average particle density on the surface plotted as a function of deposition pressure for the 250K (15.5% PEO) polymer and (b) the average aggregate area as a function of PEO composition. The deposition pressure in general increases going *down* the ordinate for a particular polymer and is plotted for the AFM data shown in Figure 2. Open squares are the ideal values calculated from the empirically determined PS sizes multiplied by the aggregation number.

spreading are quite stable and resistant to further aggregation.

Conclusion

Preparation of films from PS−PEO diblocks with greater than ∼10 wt % PEO at the air−water interface is a valuable methodology. Unlike at solid−liquid interfaces, the number of molecules per unit of area can be continuously and controllably varied for a particular diblock. Selecting the appropriate region on the phase diagram controls the spacing of the resultant aggregates formed by LB deposition on the solid substrate. Below the two- to three-dimensional phase transition of the PEO, the surface density of the polymers is observed to be linear with respect to the deposition pressure due to the linearity of the compression isotherm in that region. For a particular spreading solution concentration, the spontaneous aggregation number is determined by the relative percent of PEO in the diblock, is independent of the deposition pressure, and is thus constant for a given polymer asymmetry in this regime. This method of preparing films of controlled spacing is straightforward and elegant in its simplicity, yet a wealth of patterns and control lie in this and other ranges of the phase diagram.

Acknowledgment. This work was supported by the National Science Foundation (DMR and DUE) and through a PECASE award sponsored by the DOE/DP.

References and Notes

(1) Aksay, I. A.; Trau, M.; Manne, S.; Honma, I.; Yao, N.; Zhou, L.; Fenter, P.; Eisenberger, P. M.; Gruner, S. M. *Science* **1996**, *273*, 892−898.
(2) Fasolka, M. J.; Harris, D. J.; Mayes, A. M.; Yoon, M.; Mochrie, S. G. J. *Phys. Rev. Lett.* **1996**, *79*, 3018−3021.
(3) Mayes, A. M.; Kumar, S. K. *MRS Bull.* **1997**, Jan, 43−47.
(4) Karim, A.; Slawecki, T. M.; Kumar, S. K.; Douglas, J. F.; Satija, S. K.; Han, C. C.; Russell, T. P.; Liu, Y.; Overney, R.; Sokolov, J.; Rafailovich, M. H. *Macromolecules* **1998**, *31*, 857−862.
(5) Koutsos, V.; Van der Vegte, E. W.; Pelletier, E.; Stamouli, A.; Hadziioannou, G. *Macromolecules* **1997**, *30*, 4719−4726.
(6) Spatz, J. P.; Möller, M.; Noeske, M.; Behm, R. J.; Pietralla, M. *Macromolecules* **1997**, *30*, 3874−3880.
(7) Meiners, J. C.; Quintel-Ritzi, A.; Mlynek, J.; Elbs, H.; Krausch, G. *Macromolecules* **1997**, *30*, 4945−4951.
(8) Stamouli, A.; Pelletier, E.; Koutsos, V.; van der Vegte, E.; Hadziioannou, G. *Langmuir* **1996**, *12*, 3221−3224.
(9) Yeung, C.; Balazs, A. C.; Jasnow, D. *Macromolecules* **1993**, *26*, 1914−1921.
(10) Zhulina, E. B.; Singh, C.; Balazs, A. C. *Macromolecules* **1996**, *29*, 6338−6348.
(11) Ulman, A. In *An Introduction to Ultrathin Organic Films from Langmuir−Blodgett to Self-Assembly*; Academic Press: New York, 1991.
(12) PEO is chosen as the surface-active agent rather than the potentially more stable polyelectrolyte because the compression isotherms are more straightforward to interpret and because the nonionic aggregates can pack more tightly together due to the lack of Coulombic repulsions.
(13) Li, Z.; Zhao, W.; Quinn, J.; Rafailovich, M. H.; Sokolov, J.; Lennox, R. B.; Eisenberg, A.; Wu, X. Z.; Kim, M. W.; Sinha, S. K.; Tolan, M. *Langmuir* **1995**, *11*, 4785−4792.
(14) Zhu, J.; Eisenberg, A.; Lennox, R. B. *J. Am. Chem. Soc.* **1991**, *113*, 5583−5588.
(15) Li, S.; Hanley, S.; Khan, I.; Varshney, S. K.; Eisenberg, A.; Lennox, R. B. *Langmuir* **1993**, *9*, 2243−2246.
(16) Zhu, J.; Eisenberg, A.; Lennox, R. B. *Macromolecules* **1992**, *25*, 6547−6555.
(17) Zhu, J.; Eisenberg, A.; Lennox, R. B. *Macromolecules* **1992**, *25*, 6556−6562.
(18) Bjisterbosch, H. D.; de Haan, V. O.; de Graaf, A. W.; Mellema, M.; Leermakers, F. A. M.; Cohen Stuart, M. A.; van Well, A. A. *Langmuir* **1995**, *11*, 4467−4473.
(19) Dewhurst, P. F.; Lovell, M. R.; Jones, J. L.; Richards, R. W.; Webster, J. R. P. *Macromolecules* **1998**, *31*, 7851−7864.
(20) Li, Z.; Zhao, W.; Liu, Y.; Rafailovich, M. H.; Sokolov, J.; Khougaz, K.; Eisenberg, A.; Lennox, R. B.; Krausch, G. *J. Am. Chem. Soc.* **1996**, *118*, 10892−10897.
(21) Barentin, C.; Muller, P.; Joanny, J. F. *Macromolecules* **1998**, *31*, 2198−2211.
(22) Goncalves da Silva, A. M.; Filipe, E. J. M.; d'Oliviera, J. M. R.; Martinho, J. M. G. *Langmuir* **1996**, *12*, 6547−6553.
(23) Fauré, M. C.; Bassereau, P.; Lee, L. T.; Menelle, A.; Lheveder, C. *Macromolecules* **1999**, *32*, 8538−8550.
(24) Fauré, M. C.; Bassereau, P.; Carignano, M. A.; Szleifer, I.; Gallot, Y.; Andelman, D. *Eur. Phys. J. B* **1998**, *3*, 365−375.
(25) Gragson, D. E.; Jenson, J. E.; Baker, S. M. *Langmuir* **1999**, *15*, 6127−6131.
(26) Kumaki, J. *Macromolecules* **1988**, *21*, 749−755.
(27) Zhu J.; Lennox, R. B.; Eisenberg, A. *Langmuir* **1991**, *7*, 1579−1584.
(28) Goncalves da Silva, A. M.; Simões Gamboa, A. L.; Martinho, J. M. G. *Langmuir* **1998**, *14*, 5327−5330.

MA992029X